Langmuir soliton stability and collapse in a weak magnetic field

Lj. R. Hadžievski and M. M. Škorić
The Boris Kidrič Institute of Nuclear Sciences, P.O.B. 522, 11001 Belgrade, Yugoslavia

A. M. Rubenchik, E. G. Shapiro, and S. K. Turitsin
Institute of Automation and Electrometry, Siberian Branch, U.S.S.R. Academy of Sciences, 630090 Novosibirsk, U.S.S.R.

(Received 5 January 1990)

A detailed study of the linear stability and nonlinear wave collapse of Langmuir solitons in a weakly magnetized plasma is performed. An analytical investigation of the linear soliton instability with respect to long-wavelength transverse perturbation versus magnetic field effect is presented. For a more complete understanding of the growth-rate structure, a numerical solution of the eigenvalue problem that corresponds to the model equations is obtained and compared with analytical predictions. Comparison with earlier results is given. Furthermore, numerical results obtained by a direct simulation method in two dimensions are also presented. In a linear regime, detailed agreement with the results of the corresponding eigenvalue problem is found. In the nonlinear regime of the soliton instability all considered cases exhibit a collapse dynamics. Moreover, in the developed, highly nonlinear stage of the soliton collapse, self-similar behavior consistent with a "weak" collapse regime is found.

I. INTRODUCTION

One-dimensional stationary localized solitonlike wave structures are understood to be the basic elements of strong plasma turbulence. In one-dimensional systems solitons are stable, evolving rapidly from an arbitrary initial plasma state, and therefore they determine the basic features of the emerging plasma turbulence. However, in real plasmas, as a rule, solitons appear to be unstable with respect to transverse perturbations.[1] In a nonlinear stage of evolution, this instability often leads to a soliton collapse, a unique nonlinear wave phenomenon of the formation of a singularity in a finite time. Accordingly, the appearance of the collapsing nonstationary wave structures (cavities) that exhibit a rapid field growth followed by an intensive spatial localization (self-focusing) results in a qualitative change of the turbulence character.[2] The dispersion relation describing linear Langmuir waves in a weak magnetic field has a form

$$\omega_k=\omega_{pe}\left[1+\tfrac{3}{2}k^2r_{\mathrm{De}}^2+\frac{1}{2}\frac{\omega_{ce}^2}{\omega_{pe}^2}\frac{k_\perp^2}{k^2}\right], \tag{1.1}$$

where ω_{ce} and ω_{pe} ($\omega_{ce}\ll\omega_{pe}$) are the electron cyclotron and the electron plasma frequency, respectively, r_{De} is the Debye radius, and $k_\perp$ is the wave number component transverse to the magnetic field. It is evident that the transverse perturbation increases the wave frequency and is therefore energetically unfavorable. Accordingly, unstable modes should only correspond to long-wavelength transverse perturbations, with a frequency increase on the order of the instability growth rate. Moreover, a magnetic field increase results in an increase of the frequency of transverse oscillations and appears as a stabilizing factor.

Soliton instability in a weak magnetic field was studied in Ref. 3. It was shown that for moving solitons with a velocity $V/v_t>\omega_{ce}/\omega_{pe}$ (v_t is the electron thermal velocity) the magnetic field produces no changes in the behavior of the soliton instability apart from increasing the transverse instability length scales, according to

$$l_\perp\sim l_0\frac{\omega_{ce}^2}{\omega_{pe}^2}\frac{l_0}{r_{\mathrm{De}}},$$

where $l_0\sim(8\pi nT/E_0^2)^{1/2}$ is the soliton characteristic length.

In the opposite limit, the case of a standing soliton ($V=0$) in the long-wavelength region for the instability growth rate (γ), the following analytical solution of the corresponding eigenvalue problem[2] was obtained

$$\gamma=2\omega_{pe}\left[\left(\frac{E_0^2}{8\pi nT}\right)[12-7\zeta(3)]-\frac{21}{4}\zeta(3)\frac{\omega_{ce}^2}{\omega_{pe}^2}\right]k_\perp^2r_{\mathrm{De}}^2, \tag{1.2}$$

where

$$\zeta(x)=\sum_n n^{-x}$$

is Riemann's zeta function.

At first sight, it seems that for sufficiently large values ($\omega_{ce}^2/\omega_{pe}^2>0.43E_0^2/8\pi nT$) the magnetic field stabilizes the linear instability. However, instability may reappear if one takes into account the next terms in the expansion in transverse wave numbers $k_\perp$. The dispersion relation (1.2) in the limit $k_\perp\to0$ turns into a marginally stable mode corresponding to a small variation of the soliton amplitude. On the other hand, the expression (1.2) by itself does not appear to be sufficiently exact. In the treatment[1,3] only the first term in the expansion $\gamma(k_\perp)$ was

calculated. Moreover, the existence and solvability of the perturbation scheme, typically has not been proved, nor was the convergence of the series expansion.

Numerical results obtained by Rowland[4] indicate that the magnetic field is unable to stabilize the soliton instability. Yet, these results are based only on a few values of the parameters, so it is unclear if other regions of soliton stability exist. The influence of the magnetic field on the growth rate structure and on the transverse instability length scales remains a very important issue. These characteristics would give us an opportunity to estimate the parameters of the emerging collapsing Langmuir wave packets. The magnetic field effect on the collapse of Langmuir wave packets for different model equations has been a subject of earlier studies.[5–8]

In this paper, we present a detailed study of the influence of the magnetic field on the soliton stability. First, we formulate the basic model equation and discuss the physical background of the problem. Based on the variational principle, we present an analytical investigation of the growth rate structure in a linear regime for finite values of the transverse perturbation wave number. Then we give results of the numerical solution of the corresponding eigenvalue problem. We have obtained a complete spectral structure of the growth rate and corresponding eigenfunctions. Somewhat unexpectedly, the calculated form of $\gamma(k_\perp)$ does not agree with the analytically obtained equation (1.2). We discuss the possible reasons for this discrepancy due to the inadequate accuracy of the perturbation treatment. Finally, the last section is devoted to the nonlinear stage of the soliton instability, which exhibits a soliton collapse. In order to study the magnetic field effect on the nonlinear stage of the soliton instability we have performed direct numerical simulations in two dimensions (2D). In the linear regime we find detailed agreement with the results of the corresponding eigenvalue problem. In the nonlinear regime all considered cases exhibit collapse dynamics. Moreover, in the developed, highly nonlinear stage of the soliton collapse, self-similar behavior consistent with a "weak" collapse regime is found. Our work differs from the earlier studies on Langmuir collapse[5–8] in terms of model equation, initial conditions (soliton) level of nonlinearity and observed phenomena.

II. BASIC EQUATIONS

Nonlinear evolution of Langmuir waves in a weak magnetic field is conveniently described by a time-averaged dynamical equation for the envelope of the high-frequency potential ψ, which in dimensionless units

$$t\rightarrow\frac{3}{2}\frac{M}{m}\omega_{pe}^{-1}t,\quad \mathbf{r}\rightarrow\frac{3}{2}\left[\frac{M}{m}\right]^{1/2}r_{\mathrm{De}}\mathbf{r},\quad \psi\rightarrow\frac{T}{e}(12)^{1/2}\psi$$

reads[2]

$$\Delta(i\psi_t+\Delta\psi)-\sigma\Delta_\perp\psi+\nabla(|\nabla\psi|^2\nabla\psi)=0\ , \tag{2.1}$$

where $\sigma=\frac{3}{4}\omega_{ce}^2/\omega_{pe}^2 M/m$, M and m are the ion and the electron mass, respectively. The external magnetic field B ($\omega_{ce}=eB/mc$) is in the x direction while the dimensionless equation (2.1) is valid for $\sigma\ll\frac{3}{4}M/m$. The linear part of (2.1) corresponds to the dispersion relation (1.1) while the nonlinear term is described through a static plasma response to the ponderomotive force action. We assume that the characteristic nonlinear time scales are slower than the ion-sound motions. The above is justified in a small amplitude region $E_0^2/8\pi nT<m/M$, the subsonic regime.

For more complete insight into the soliton stability problem and corresponding growth rate structure the inclusion of the ion inertia is essential (see Refs. 5–9). A detailed study of this physical problem will be presented in a separate publication. As will be seen below, the magnetic field increase results in an increase of transverse perturbation length scales. Under the assumption that the characteristic transverse length scales are sufficiently larger than longitudinal ones, the equation (2.1) substantially simplifies to[9]

$$\frac{\partial^2}{\partial x^2}(i\psi_t+\psi_{xx})-\sigma\Delta_\perp\psi+\frac{\partial}{\partial x}(|\psi_x|^2\psi_x)=0\ . \tag{2.2}$$

As mentioned above, we shall investigate stability of a planar standing soliton, as the only known analytical solution of (2.1) and (2.2)

$$\psi_0=\sqrt{2}\arctan[\sinh(\lambda x)]\exp(i\lambda^2 t)\ , \tag{2.3}$$

where λ is the soliton strength parameter.

We study the stability of (2.3) with respect to small transverse perturbations with a potential $\psi_p=f+ig$ in a form

$$f,g\sim\exp(i\lambda^2 t+\gamma\lambda^2 t+ik\lambda y),\quad k\equiv k_\perp/\lambda\ .$$

Linearizing (2.1) on the background of the soliton (2.3) and taking $x\rightarrow x\lambda$ and $\sigma\rightarrow\sigma/\lambda^2$ we obtain

$$\begin{aligned}&\gamma\left[\frac{d^2}{dx^2}-k^2\right]f+\left[\frac{d^4}{dx^4}-(1+2k^2)\frac{d^2}{dx^2}\right.\\&\qquad\left.+k^2(1+\sigma+k^2)-\frac{2k^2}{\cosh^2 x}+\frac{d}{dx}\frac{2}{\cosh^2 x}\frac{d}{dx}\right]g=0\ ,\\&-\gamma\left[\frac{d^2}{dx^2}-k^2\right]g+\left[\frac{d^4}{dx^4}-(1+2k^2)\frac{d^2}{dx^2}\right.\\&\qquad\left.+k^2(1+\sigma+k^2)-\frac{2k^2}{\cosh^2 x}+\frac{d}{dx}\frac{6}{\cosh^2 x}\frac{d}{dx}\right]f=0\ .\end{aligned} \tag{2.4}$$

The increment γ (growth rate) of instability is given by the eigenvalues of the equation (2.4) corresponding to the spatially localized eigenfunctions.

In the literature there exist standard methods of solutions for $\gamma(k)$ in the long-wavelength limit, based on the local proximity of the eigenfunctions (2.4) for neutrally stable perturbations.[1] It is evident that odd and even (with respect to x) solutions of (2.4) can be treated independently. Odd modes (antisymmetric) correspond to marginally stable soliton deformations in the long-wavelength region. However, for even (symmetric)

modes in Ref. 3, the following analytical solution was obtained:

$$\gamma^2=2k^2\{[12-7\zeta(3)]-7\sigma\zeta(3)\} . \quad (2.5)$$

Due to instability the soliton is split into a number of wave packets that each exhibit a local growth of the soliton amplitude. From the expression (2.5) it seems that for sufficiently large values of σ,

$$\sigma > \frac{12-7\zeta(3)}{7\zeta(3)} ,$$

the magnetic field stabilizes the instability. However, as already mentioned, in a real situation this might not occur. Namely, the instability may reappear in the calculations if one takes into account the next terms of the expansion in k. It seems that standard analytical methods do not appear to be successful in that case. Therefore, we shall try to investigate the structure of the growth rate $\gamma(k)$ for finite values of k by applying an approximative variational method.

III. VARIATIONAL TREATMENT OF SOLITON STABILITY

A basic idea of an approximative "brute force" treatment of a soliton instability in its nonlinear stage (see Ref. 10 and references therein) is as follows.

Equation (2.1) can be obtained by the variational principle

$$\delta S=0 , \quad (3.1)$$

where S is the action defined by

$$S=\int\int\left\{\frac{i}{2}(\nabla\psi\nabla\psi_t^*-\nabla\psi^*\nabla\psi_t)+|\Delta\psi|^2+\sigma|\nabla_\perp\psi|^2-\tfrac{1}{2}|\nabla\psi|^4\right\}d\mathbf{r}\,dt . \quad (3.2)$$

Let us substitute ψ in (3.2) as a set of trial functions with varying parameters. In our case we chose ψ in the following form:

$$\psi_0=\sqrt{2}\arctan\{\sinh[\lambda(y,t)x]\}\exp[-i\varphi(y,t)] , \quad |\lambda_{t,y}|\ll|\varphi_{t,y}| . \quad (3.3)$$

Accordingly, Eq. (3.1) reduces to a much simpler system of differential equations for λ and φ, which can be treated by standard analytical methods. However, the success of the above procedure essentially depends on our choice of trial functions. As already mentioned, an unstable mode appears as a local modulation of the soliton amplitude and phase. Our chosen trial function corresponds to such type of perturbation and should in a long-wavelength limit recover expression (2.5).

We substitute the trial function (3.3) into the action S, where after a straightforward procedure we obtain

$$S=\int\int[4\lambda\varphi_t-\tfrac{4}{3}\lambda^3+24\varphi_y^2\lambda-(\lambda_y\varphi_{yt}\lambda^{-2}-\varphi_y\lambda_{yt}\lambda^{-2}-2\varphi_y^2\varphi_t\lambda^{-1}-2\varphi_{yy}^2\lambda^{-1}-2\sigma\varphi_y^2\lambda^{-1}-2\lambda_{yy}\varphi_y^2\lambda^{-2}+4\varphi_y\varphi_{yy}\lambda_y\lambda^{-2}-2\varphi^4\lambda^{-1})I_0+4\lambda_{yy}^2\lambda^{-2}I_2]dy\,dt , \quad (3.4)$$

where

$$I_0=\int_0^\infty[\arctan(\sinh x)-\pi/2]^2dx ,$$

$$I_2=\int_0^\infty\frac{x^2}{\cosh^2 x}dx .$$

By varying the functional S over φ and λ, it is possible to derive a system of two equations (if the initial function was appropriately chosen). We limit ourself to check if in a long-wavelength limit ($k\to 0$) of the linearized version of the equations $\delta S/\delta\varphi=0$ and $\delta S/\delta\lambda=0$, one can recover the results in Ref. 3. By linearizing the equations $\partial S/\delta\varphi=0$ and $\delta S/\delta\lambda=0$ on the background of the stationary solutions $\varphi_0=t\lambda_0^2$, $\lambda_0=\text{const}$, $\varphi=\varphi_0+\delta\varphi$, $\lambda=\lambda_0+\delta\lambda$, we get

$$-4\delta\lambda_t-48\lambda_0\delta\varphi_{yy}-(2\lambda_0^{-2}\delta\lambda_{yyt}+4\lambda_0\delta\varphi_{yy}+4\lambda_0^{-2}\delta\varphi_{yyyy}-4\sigma\lambda_0^{-1}\delta\varphi_{yy})I_0=0 , \quad (3.5)$$

$$4\delta\varphi_t-8\lambda_0\delta\lambda+2\lambda^{-2}I_0\delta\varphi_{yyt}+8\lambda_0^{-3}I_2\delta\lambda_{yyyy}=0 . \quad (3.6)$$

For perturbations in a form $\delta\lambda$, $\delta\varphi\sim\exp(\gamma t+iky)$, after simple calculations we obtain the formulas for $\gamma(k)$ as

$$\gamma^2=2\frac{[12\lambda_0^2-7(\lambda_0^2+\sigma)\zeta(3)]k^2+7\zeta(3)k^4}{[1+\frac{7}{2}\zeta(3)k^2\lambda_0^{-2}]^2} . \quad (3.7)$$

It is evident that in a long-wavelength limit our result (3.7) agrees with (2.5). However, it is also obvious that the instability reappears if we take into account the higher order terms in k. The maximum growth rate depends only weakly on σ. Accordingly, generally taken, in the framework of Eq. (2.1) the magnetic field does not stabilize the soliton stability. However, based on (3.7), for sufficiently strong magnetic fields, islands (regions) of stability around

$$\sigma=\frac{12-7\zeta(3)}{7\zeta(3)}\lambda_0^2$$

should exist.

We have already emphasized that the accuracy of the above-noted variational treatment critically depends on our choice of trial functions. This procedure seems convenient to predict the rough qualitative features of the instability increment, however, hardly adequate enough to describe the fine structure of the eigenmode corresponding to (2.5).

Therefore, to single out the detailed structure of the instability increment, we have numerically solved the eigenvalue problem (2.4).

IV. NUMERICAL TREATMENT

In order to find a detailed structure of the instability increment $\gamma(k)$ it is necessary to calculate a set of eigenfunctions which vanish at infinity with the corresponding eigenvalues for γ, for different values of the perturbation wave number k and the magnetic field σ. As mentioned above, unstable modes, at least in the long-wavelength limit, correspond to a symmetric (even) type of the electric field perturbations. Accordingly, the electric potential perturbations are antisymmetric. This situation enables us to solve the system (2.4) in the interval $[0,\infty)$ with the boundary conditions

$$\left.\frac{d^4\delta\psi}{dx^4}\right|_{x=0}=\left.\frac{d^2\delta\psi}{dx^2}\right|_{x=0}=0, \quad \delta\psi=f+ig \ . \tag{4.1}$$

Further, based on (2.4) the following condition is automatically satisfied:

$$\delta\psi|_{x=0}=0 \ .$$

In order to find spatially localized (vanishing at infinity) solutions which satisfy (4.1) we have adopted the following method. On the right-hand side (rhs) of the interval $[0,R]$ $R\gg 1$, for given k, we assume the following asymptotic solution of (2.4):

$$\delta\psi=f+ig=C_1\exp(K_1x)+C_2\exp(K_2x) \ , \tag{4.2}$$

where C_1 and C_2 are the arbitrary complex constants. By making use of (4.2) as boundary conditions for (2.4) it is possible to solve the system (1.4) as a Cauchy problem and to calculate the eigenfunction $\delta\psi$ and its derivatives at the lhs of the interval (at $x=0$). As a next step, we define an auxiliary function $F(\gamma,C_1,C_2)$ in the following way:

$$F(\gamma,C_1,C_2)=[f^2(0)+f_{xx}^2(0)+f_{xxxx}^2(0)+g^2(0)+g_{xx}^2(0)+g_{xxxx}^2(0)]^{1/2} \ .$$

If F revolves at a zero point, then the obtained functions $f(x)$ and $g(x)$ appear to be the eigenfunctions and $\gamma(k)$ the corresponding eigenvalue of the system (2.4), with boundary conditions (4.1) and (4.2). The function F depends on five independent parameters. Based on a linearity of (2.4) it is possible to fix one of them, e.g., $\mathrm{Im}C_1=1$. By varying the remaining parameters we look for a minimum of the function F. The minimization is performed by the method of steepest descent, starting with arbitrary values of γ^0, C_1^0, and C_2^0. Typical maximum values for f and g were equal or larger then unity. The procedure was terminated when the value of F became smaller than 10^{-3}. In order to perform calculations in the small k region, with the slowly decaying asymptotic solutions, we have chosen a substantially larger interval of calculations $R=8$.

It has been proved that for all considered initial states a single minimum of F exists being independent on the initial conditions. Therefore, in Fig. 1 we plot the calculated spectrum $\gamma(k)$ for different values of σ. It is evident (Fig. 1) that the magnetic field increase results in a continuous change of $\gamma(k)$; its maximum shifted to the long-wavelength region while the maximum value weakly increases with σ. Accordingly, the magnetic field increase leads to growth of the transverse perturbation length scales. For larger values of $l_\perp/l_\parallel$, i.e., for larger magnetic fields (σ), which correspond to Eq. (2.2), the spectral dependence $\gamma(k)$ on the magnetic field strength appears to be universal:

$$\gamma(k,\sigma)=\gamma(k\sqrt{\sigma}) \ . \tag{4.3}$$

Our calculations indicate that the transition to this universal behavior (4.3) already appears at $\sigma=10$.

It is a very important fact that the numerically calculated spectral dependence differs qualitatively from the analytical formulas obtained in Sec. III. Namely, numerical results show that the magnetic field increase does not produce an island of stability near $k=0$; i.e., instability exists in the entire interval between $k=0$ and the cutoff (critical) value $k=k_c$. On the other hand, the spectral structure of the growth rate in the small k region considerably differs from the analytically predicted dependence $\gamma(k)\sim k$, exhibiting a nonlinear behavior according to $\gamma(k)\sim k^{1/3}$ (see Fig. 2).

The above situation convinces one that the formulation of the perturbation theory for the plasma soliton stability proposed in Refs. 1 and 3 does not appear to be sufficiently accurate. As an additional check of this problem we have performed further investigations in the region $k\to 0$. It seems obvious that for $k=0$ and $\gamma=0$ neutrally stable perturbations correspond to infinitely small variations of the soliton parameters. Accordingly, the eigenfunctions f and g of a symmetric type turn out to be

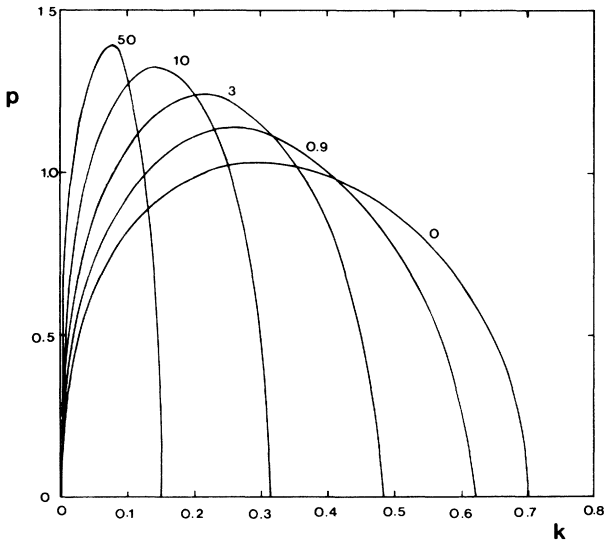

FIG. 1. Linear growth rate (p) vs transverse perturbation wave number (k) for five values of the magnetic field (σ): 0, 0.9, 3, 10, and 50.

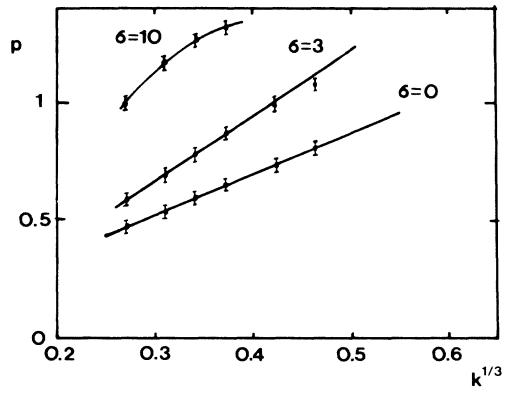

FIG. 2. Linear growth rate (p) vs transverse perturbation wave number ($k^{1/3}$) for three values of the magnetic field (σ): 0, 3, and 10.

$$f=0, \quad g=\sqrt{2}\arctan(\sinh x) . \tag{4.4}$$

Our numerically calculated solutions, as $k\to 0$, continuously assume the form of (4.4).

Furthermore, we study the spectral behavior near the cutoff value k_c. Solutions of the eigenvalue problem (2.4) for $k\neq 0$ and $\gamma=0$ were obtained in an independent way. It appears that two types of solutions exist. The first one, with the critical (cutoff) wave number $k_c=1-\sigma$, if $k\neq k_c$ turns into a stable mode ($\gamma^2<0$). The second type corresponds to an unstable branch (for $\sigma=0$ and $k_c\cong 0.7$) with a continuous transition for $k\neq k_c$ to a solution of the complete system (2.4).

In order to check the accuracy of our numerical method we have investigated the soliton instability in the framework of the nonlinear Schrödinger (NLS) equation. The calculated spectral form of $\gamma(k)$ coincides with the one found in Ref. 11. In the case of the NLS equation, the soliton stability problem for a small k is solvable with the perturbation theory[1] to any order of expansion, therefore $\gamma\sim k$ for $k\to 0$, as was confirmed in our calculations.

Moreover, we have attempted to analytically construct a novel perturbation scheme which for $k\to 0$ should correctly recover the results of the above numerical calculations. We look for a solution of (2.4) in a form of series expansion for a small k values

$$\begin{aligned}
&\gamma = Ak^{1/3}+\cdots , \\
&g = g_0+k^{2/3}g_{2/3}+k^{4/3}g_{4/3}+\cdots \\
&\quad \equiv g'_0+g'_{2/3}+g'_{4/3}+\cdots , \\
&f = k^{1/3}(f_{1/3}+k^{2/3}f_{3/3}+k^{4/3}f_{5/3}+\cdots) \\
&\quad \equiv f'_{1/3}+f'_{3/3}+f'_{5/3}+\cdots .
\end{aligned} \tag{4.5}$$

In the first order of the perturbation theory we get

$$\frac{d}{dx}H_+\frac{d}{dx}f'_{1/3}=\gamma\frac{d^2}{dx^2}g'_0 . \tag{4.6}$$

Further, to successive orders one obtains

$$\begin{aligned}
&\frac{d}{dx}H_-\frac{d}{dx}g'_{2/3}=-\gamma\frac{d^2}{dx^2}f'_{1/3} , \\
&\frac{d}{dx}H_+\frac{d}{dx}f'_{3/3}=\gamma\frac{d^2}{dx^2}g'_{2/3} , \\
&\frac{d}{dx}H_-\frac{d}{dx}g'_{4/3}=-\gamma\frac{d^2}{dx^2}f'_{3/3} , \\
&\frac{d}{dx}H_+\frac{d}{dx}f'_{5/3}=\gamma\frac{d^2}{dx^2}g'_{4/3} ,
\end{aligned} \tag{4.7}$$

where

$$\begin{aligned}
H_+ &= \frac{d^2}{dx^2}-1+\frac{6}{\cosh^2 x} , \\
H_- &= \frac{d^2}{dx^2}-1+\frac{2}{\cosh^2 x} .
\end{aligned}$$

Finally, at the sixth order, we come across the terms proportional to k^2:

$$\frac{d}{dx}H_-\frac{d}{dx}g'_{6/3}+k^2\left[-\frac{d^2}{dx^2}+\sigma+1-\frac{2}{\cosh^2 x}\right]g_0 +\gamma\frac{d^2}{dx^2}f'_{5/3}=0 . \tag{4.8}$$

In that way, so far as $f'_{5/3}\sim\gamma^5$, we have constructed the perturbation scheme for which $\gamma\sim k^{1/3}$. Although operators H_+ and H_- and their inverse counterparts are well defined, a fact that, in principle, should allow the derivation of $f'_{5/3}(x)$, the proof of the convergence of the above perturbation scheme is rather complex. A particular point lies in the fact that the expansion for a small k is justified only in the region $|x|\ll 1/k$. This is connected with a slow decay of the solution of the complete system (2.4) $f,g\sim\exp(-kx)$. Naturally, that is a reason why we try to check the proposed scheme upon our numerical calculations. It is evident from Fig. 2 that the dependence $\gamma\sim k^{1/3}$ is obeyed with a high degree of accuracy

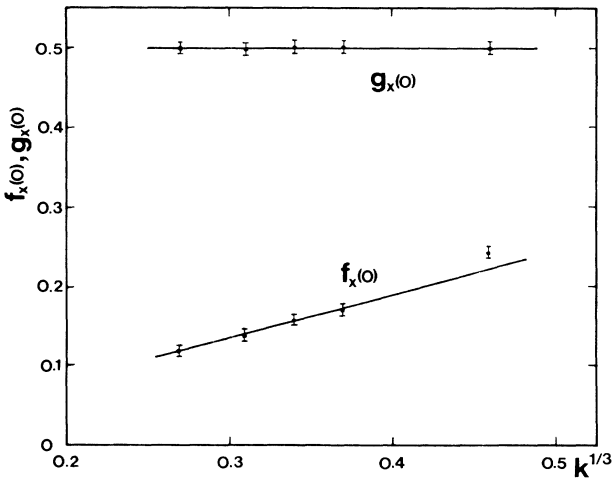

FIG. 3. Spatial derivatives of eigenfunctions (f,g) at $x=0$ vs transverse perturbation wave number ($k^{1/3}$).

for small k values. The deviation from the above dependence, for large σ, comes from the fact that in this case, as $\gamma = f(k\sqrt{\sigma})$, the expansion is justified for substantially smaller values of k. In Fig. 3 we plot the dependence of $dg/dx|_{x=0}$ and $df/dx|_{x=0}$ on $k^{1/3}$. As expected from the expansion (4.5), $g_x(0) = \text{const}$ and $f_x(0) = Bk^{1/3}$. In this way, our numerical results give strong support for the proposed perturbation scheme.

V. NONLINEAR STAGE OF THE SOLITON INSTABILITY

Further, we discuss a nonlinear stage of the soliton instability. In an isotropic plasma, in a linear regime, this instability results in a transverse modulation of the soliton amplitude. The nonlinear growth of the perturbation leads to a soliton breakup into a number of collapsing wave packets (Langmuir cavities).[12] Therefore, in our problem, it is expected that the magnetic field might substantially affect this nonlinear stage of the soliton instability (see Refs. 5–8).

In Fig. 4 we plot the eigenfunctions of the system (2.4) calculated in Sec. IV that correspond to the maximum linear growth rate for different values of the magnetic field. It is evident that the increase of σ does not bring a qualitative change in a structure of the growing perturbations. Therefore, it seems reasonable to expect that the magnetic field growth just increases the transverse length scales of the wave packet leaving all basic qualitative features of the collapse process preserved.

In order to investigate the soliton instability, in particular, in its highly nonlinear (developed) stage, we have further performed a direct numerical simulation of Eqs. (2.1) and (2.2) in two dimensions (2D). We have used the spectral Fourier method with respect to the space coordinates with an explicit time integration scheme. The instability development was studied by imposing initial conditions in a form of the standing planar soliton (2.3) periodically perturbed in a transverse direction. For sufficiently large values of σ the calculations based on (2.1) and (2.2) produce very close results.

Moreover, the direct simulation results are checked against those obtained in Sec. IV of this paper. In the initial stage, where instability exhibits an exponential growth of the perturbation, we have chosen sufficiently small initial perturbation levels. We have used periodic boundary conditions (L_x, L_y), a numerical grid of 32×32 (checked upon 64×64) points, a time step of 0.001 and the perturbation level $\epsilon = 1\%$, with regularly checking the conserved integrals of (2.1) and (2.2), i.e., the plasmon number (N) and the Hamiltonian (H). As compared to Pereira, Sudan, and Denavit[12] the perturbation level ϵ was decreased until the growth rate γ has become independent on ϵ. We have performed runs with different values for k and σ. However, in the range of small perturbation wave numbers ($k < 0.2$) the grid resolution appears to be insufficient for accurate calculations. In Fig. 5 we compare the direct simulation results for $\gamma(k)$ with the results of Sec. IV, i.e., numerical solutions of the eigenvalue problem (2.4). As seen on inspection the results based on these two essentially independent methods of solution show satisfactory agreement. In particular, the results coincide for the values near to the cutoff wave numbers.

The direct simulation results have confirmed that all linearly unstable solitons, independently of the magnetic field strength and the perturbation wave number, in their nonlinear stage enter a collapse phase. This result is consistent with the earlier work of Goldman and coworkers[5,6] concerning the collapse of Langmuir wave packets in a weak magnetic field with full ion dynamics. In order to illustrate this, we show typical time plots in Fig. 6 of the early collapse, which exhibit the basic collapse features: the initial localization, subsequent explosive wave amplitude growths connected with a rapid decrease of the spatial dimensions resulting in high wave energy densities. The earlier results on soliton break up

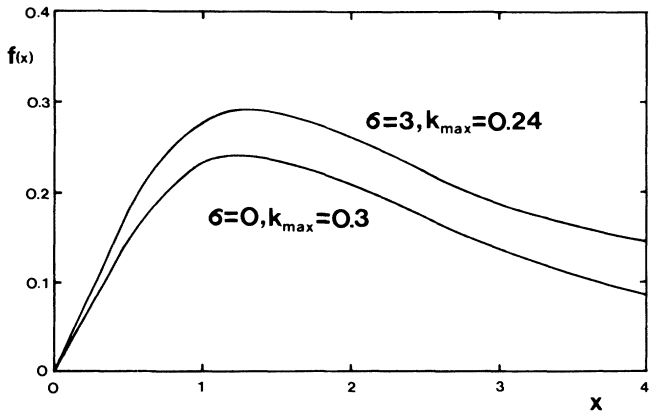

FIG. 4. Eigenfunction $[f(x)]$ for $\sigma = 0$ and $\sigma = 3$.

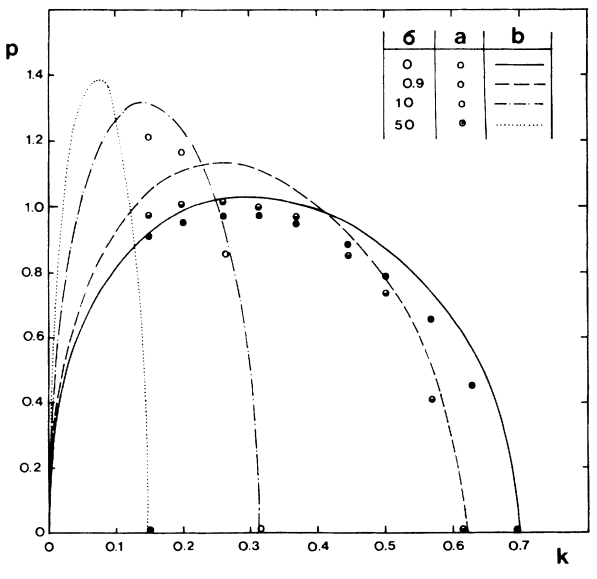

FIG. 5. Linear growth rate (p) vs transverse perturbation wave number (k) for four values of the magnetic field (σ): 0, 0.9, 10, and 50. (a) Direct 2D simulation method, (b) solution of the spectral problem.

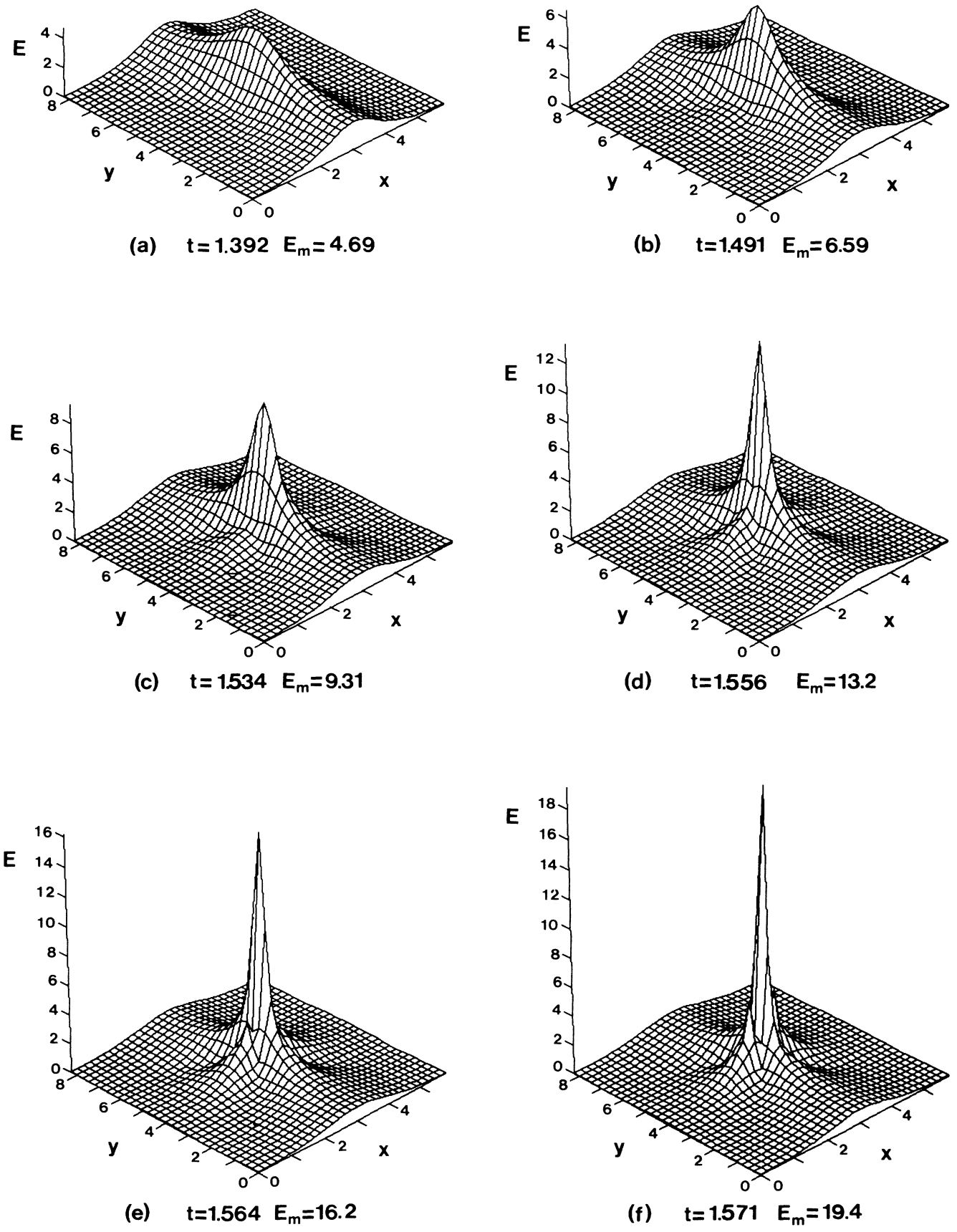

FIG. 6. Space-time dependence of the electric field amplitude (E).

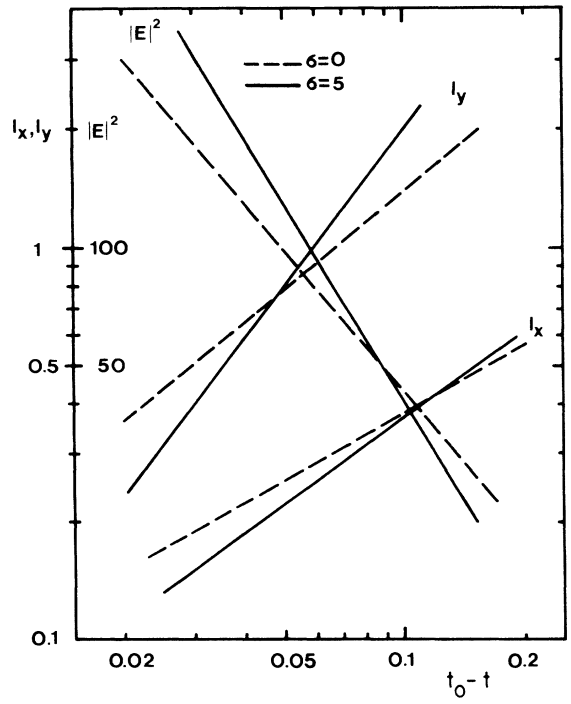

FIG. 7. Characteristic spatial scales (l_x, l_y) and the maximum electrostatic energy density ($|E|^2$) as a function of the time interval to the collapse time (t_0). Dashed lines denote $\sigma=0$ and solid lines denote $\sigma=5$.

and subsequent collapse in an unmagnetized plasma[12] were readily recovered in our simulations for $\sigma=0$.

An important characteristic of the collapsing wave packet is its eccentricity (Fig. 7), i.e., the elongation ratio l_x/l_y. This quantity defines the energy content trapped inside the cavity, which is of considerable importance concerning the final collapse stage and the ultimate energy dissipation. Generally taken, there possibly exist solutions with various degrees of eccentricity,[13] also depending on the way they were initially formed.

Self-similarity and collapse regimes

Let us further discuss a highly nonlinear, developed stage of the collapse. A general scenario was proposed in the early work of Krasnosel'skikh and Sotnikov[9] which was based on an analytical study of a version of Eq. (2.2), which takes into account a full ion inertial response. The above is necessary in the so-called supersonic regime ($E_0^2/8\pi n_0 T > m/M$) of the magnetized Langmuir wave collapse.

In the early stage of the soliton collapse, as long as $\omega_{ce}/\omega_{pe} \gg k r_{\mathrm{De}}$, the transverse dimensions of the collapsing wave packet are substantially larger than the longitudinal ones, forming highly elongated, dipole field structures. During the collapse process the transverse length scale of the cavity decreases more rapidly than the longitudinal one and therefore, when $k r_{\mathrm{De}} \sim \omega_{ce}/\omega_{pe}$, these two scales become of the same order. Accordingly, in the later stage, the magnetic field is not expected to influence the collapse development.[9] However, it is still believed that in the final collapse stage magnetic field might possibly make an effect on the cavity structure and its energy content. Indeed, our simulation results seems to point in the same direction (*vide infra*), i.e., that in the final stage, the cavity form and the trapped energy depend on the magnetic field strength.

Further, we investigate the potential self-similar time behavior of the wave collapse process in its developed stage. More recent studies of the wave collapse have shown that a collapse process, as a unique nonlinear phenomenon of the formation of a singularity in a finite time, can be developed through two different collapse regimes: *weak* and *strong*. Zakharov and Kuznetsov[14] for the case of the NLS equation and Kuznetsov and Škorić[15] for the nonlinear upper-hybrid and lower-hybrid waves have shown that during the *strong* collapse regime the trapped wave energy through the collapse stage remains finite and the wave radiation from the cavity is absent. On the other hand, in the *weak* regime, which formally preserves zero energy into the final collapse stage, wave radiation is present. In the framework of Eq. (2.2) it has been shown that two regimes, *weak* and *strong*, exist. Both regimes near the singularity can be described by a general self-similar ansatz in the form

$$\psi(\mathbf{r},t)=\frac{1}{(t_0-t)^{a+ip}} f\left[\frac{x}{(t_0-t)^b}, \frac{\mathbf{r}_\perp}{(t_0-t)^c}\right], \tag{5.1}$$

where a, b, c, and p are the real parameters. This means that the cavity dimensions scale as

$$l_x=(t_0-t)^b, \quad l_\perp=(t_0-t)^c . \tag{5.2}$$

The number of waves localized in the cavity (N^{cav}) depends on time (in two dimensions) as

$$N^{\mathrm{cav}}=\int \left|\frac{\partial\psi}{\partial x}\right|^2 d\mathbf{r} \sim (t_0-t)^{2a-b+c}, \quad 2a-b+c\geq 0 , \tag{5.3}$$

where for a *strong* collapse N^{cav} should remain constant, while for a *weak* collapse N^{cav} goes to zero as collapse reaches the singularity.

We return to the early collapse stage when $\omega_{ce}/\omega_{pe} \gg k r_{\mathrm{De}}$. In this case, a simplified version of the nonlinear equations (2.2) is appropriate which accepts the following self-similar substitution:[9]

$$\psi(\mathbf{r},t)=\frac{1}{(t_0-t)^{ip}} f\left[\frac{x}{(t_0-t)^{1/2}}, \frac{\mathbf{r}_\perp}{(t_0-t)}\right], \tag{5.4}$$

where the corresponding cavity dimensions scale like

$$l_x=(t_0-t)^{1/2}, \quad l_\perp=(t_0-t) .$$

However, the above self-similar ansatz describes the *weak* collapse process with a cavity plasmon number (N^{cav}) which decreases in time as

$$N^{\mathrm{cav}}=\int \left|\frac{\partial\psi}{\partial x}\right|^2 d\mathbf{r} \sim (t_0-t)^{1/2}$$

for the 2D case.

The numerical simulation of an axially symmetric version of the Krasnosel'skikh equation presented in Ref. 16 has seemed to support the above general picture.[9] However, conclusions concerning the late collapse stage, when the disappearing magnetic field effect supposingly switches the collapse to an isotropic type of evolution, are somewhat of a speculative nature.

In order to check the self-similar character of the collapse evolution consistent with (5.1), based on our 2D numerical simulation results, we vary t_0 to find the best fit for the time evolution of the maximum electric field amplitude, for different values of the magnetic field $\sigma=0$, 5, 10, and 15. From (5.1), the maximum electric field amplitude squared scales like

$$|E_{\max}|^2 \sim \frac{1}{(t_0-t)^{\alpha}}, \quad \alpha=2a+2b \ . \tag{5.5}$$

Our results indicate that the self-similar evolution is exhibited also for smaller values of σ including $\sigma=0$, with a slope $\alpha=1.2$, which is in agreement with the earlier results of Pereira, Sudan, and Denavit.[12] For $\sigma=15$ they come close to the analytical predictions[15] ($\alpha=2$) based on Eq. (2.2). In Fig. 7 we plot in a double-logarithmic scale, the time variation of the maximum amplitude (5.5) and characteristic spatial dimensions of the collapsing cavity for $\sigma=0$ and $\sigma=5$. The self-similar behavior is evident, although with a different slope:

$$\alpha_0 \cong 1.20 \quad (\sigma=0), \quad \alpha_5 \cong 1.74 \quad (\sigma=5) \ .$$

Transverse length scales grow faster than longitudinal ones, resulting in that the initial dipole field structure tends to be symmetrized. The above process gets more pronounced with the magnetic field increase.

By calculating the parameters a, b, and c from Fig. 7 we readily find the time dependence of the plasma number ($N^{\rm cav}$), which based on (5.3) turns out to decrease in time, as

$$N_0^{\rm cav} \sim (t_0-t)^{0.20}, \quad N_5^{\rm cav} \sim (t_0-t)^{0.36} \ ,$$

which defines a *weak* type of collapse.

However, the self-similar features of the described collapse processes, were studied in a time interval restricted to increase of the energy density on approximately two orders of magnitude. Therefore, the later stages of the collapse, closer to the singularity, might exhibit somewhat altered type of dynamics.

As a general picture, our simulation seems to indicate an early collapse development corresponding to a weak collapse regime. Possibly, this comes from the fact that in order to approach other, the so-called (ultra) strong collapse[18] regime, much larger inertial interval seems necessary.

The energy content of the collapsing wave structure is of a considerable physical interest. Namely, the results indicate an altered effective absorption rate, i.e.,

$$[(k_0 r_{\rm De})/(\omega_{ce}/\omega_{pe})]^{1/2} \sim (E_0^2/8\pi nT)^{1/2}\omega_{pe}/\omega_{ce}$$

times the absorption rate for an isotropic plasma, corresponding to the increased level of the strong Langmuir turbulence. However, a possibility of an experimental insight in such physical situation would be of great scientific value.

Finally, it was only recently understood that the ultimate "burn out" process of the collapsing wave packets is expected to dissipate a finite amount of the wave energy. Namely, the structure of the weak collapse (conserving zero energy) seemed to indicate that the final stage should allow only an infinitely small value of the dissipated energy. However, in reality one expects a different situation. Recent refinements in the wave-collapse theory have indicated a possibility[2] of a collapse process formed as a long-living spatially localized narrow core (hot spot) close to a singularity, which entrains the wave energy from the surrounding region (black hole effect). Such an effect was variably named as a "funnel effect,"[2] "nucleation process,"[13] or "distributed collapse."[17] Accordingly, in our case, the solution (5.1) is supposingly valid only in a thin region close to the singularity. At larger distances, different type of a solution is formed providing a continuous energy influx into the singularity. More simply, in such a weak collapse dynamics a type of a "funnel" is formed entraining the energy from the outer regions.

For our Eq. (2.2) this funnel is of an anisotropic structure. Anisotropic bi-self-similar[19] collapse solution describing a finite energy capture into an anisotropic funnel has been obtained only recently.[18]

[1] V. E. Zakharov, A. M. Rubenchik, Zh. Eksp. Teor. Fiz. **65**, 997 (1973) [Sov. Phys.—JETP **38**, 494 (1974)]; E. A. Kuznetsov, V. E. Zakharov, and A. M. Rubenchik, Phys. Rep. **142**, 103 (1986).

[2] V. E. Zakharov, in *Handbook of Plasma Physics*, edited by A. A. Galeev and R. N. Sudan (North-Holland, Amsterdam, 1983), Vol. 2.

[3] M. A. Brezovskii, A. I. Dyachenko, and A. M. Rubenchik, Zh. Eksp. Teor. Fiz. **88**, 1191 (1985) [Sov. Phys.—JETP **61**, 701 (1985)].

[4] H. L. Rowland, Phys. Fluids **28**, 150 (1986).

[5] M. V. Goldman, J. C. Weatherall, and D. R. Nicholson, Phys. Fluids **24**, 668 (1981).

[6] J. P. Sheerin, J. C. Weatherall, D. R. Nicholson, G. L. Payne, M. V. Goldman, and P. J. Hansen, J. Atmos. Terr. Phys. **44**, 1043 (1982).

[7] H. L. Pecseli, J. J. Rasmussen, and K. Thomsen, Phys. Rev. Lett. **99A**, 175 (1983).

[8] M. J. Giles, Phys. Rev. Lett. **47**, 1606 (1981).

[9] V. V. Krasnosel'skikh and V. I. Sotnikov, Fiz. Plazmy **3**, 872 (1977) [Sov. J. Plasma Phys. **3**, 491 (1977)].

[10] B. A. Trubnikov and S. K. Zhdanov, Phys. Rep. **155**, 137 (1987).

[11] P. A. Jansenn and J. J. Rasmussen, Phys. Fluids **26**, 1297 (1983).

[12] N. R. Pereira, R. N. Sudan, and J. Denavit, Phys. Fluids **20**, 936 (1977).

[13] P. A. Robinson, D. L. Newman, and M. V. Goldman, Phys. Rev. Lett. **62**, 2132 (1989).

[14] V. E. Zakharov and E. A. Kuznetsov, Zh. Eksp. Teor. Fiz. **91**,

1310 (1986) [Sov. Phys.—JETP **64**, 773 (1986)].
[15]E. A. Kuznetsov and M. M. Škorić, Phys. Rev. A **38**, 1422 (1988).
[16]A. S. Lipatov, Pis'ma Zh. Eksp. Teor. Phys. **26**, 516 (1977) [JETP Lett. **26**, 337 (1977)].
[17]S. V. Vlasov, L. I. Piskunova, and V. I. Talanov, in *Proceedings of the Third Workshop on Nonlinear and Turbulent Processes in Physics, Kiev, 1987,* edited by V. M. Chernousenko (Naukova Dumka, Kiev, 1987), Vol. 2, p. 210.
[18]E. A. Kuznetsov and S. K. Turitsyn, Phys. Lett. A (to be published).
[19]V. M. Malkin, Pis'ma Zh. Eksp. Teor. Fiz. **48**, 603 (1988) [JETP Lett. **48**, 653 (1988)].